Torsion in Microstructure Hollow Thick-Walled Circular Cylinder Made up of Orthotropic Material

S. Yadav [*], S. Sharma

Department of Mathematics, Jaypee Institute of Information Technology, Noida, India

ABSTRACT

In this paper, a numerical solution has been developed for hollow circular cylinders made up of orthotropic material which is subjected to twist using micro polar theory. The effect of twisting moment and material internal length on hollow thick-walled circular cylinder made up of micro polar orthotropic material is investigated. Finite difference method has been used to exhibit the influence of shear moduli and material internal length on shear stresses and couple stresses. It is found that the effect of small characteristic length on shear stresses is negligible and couple stresses present its significance when characteristic length is large in solid particle. The behavior of couple stresses are nonlinear for large internal length while for small internal length couple stresses are linear in nature except near the free boundaries. Torsion in hollow cylinder made up of micro polar orthotropic play vital role in the presence of cracks and holes. Therefore, torsional analysis of hollow cylinder plays important role in the field of biomechanics.

© 2018 IAU, Arak Branch. All rights reserved.

Keywords: Elastic; Orthotropic; Micro polar; Characteristics length; Twist; Couple stress.

1 INTRODUCTION

$\mathbf{T}$HE classical theory of elasticity consider material continua as simple point continua with points having three degrees of freedom of displacement. Such a model may be insufficient to describe the behavior of solid materials endowed with an internal structure, as in the case of block structure granular materials [1] and biological tissues [2] etc. Therefore, Eringen [3, 4] introduced the micro polar theory to study the concept of length of scale in microstructure. Due to introduction of internal length, the new measure of deformation has been introduced. In addition to three degree of freedom of displacement, the micro polar theory owns three additional independent degree of freedom related to the rotation of each particle which need not coincide with the macroscopic rotation of the continuum at the same point. Many engineering materials exhibit micro behavior i.e. honeycombs, trusses and platelet composites etc. Moreover, materials like soils, human bones and polyfoams are also considered as micro polar material. Altenbach [5], Gauthier and Jahsman [6] and Merkel et al. [7]. Roman and Lev [8] presented the finite element modeling of bending of micro polar elastic plates and obtained numerical results for plates of different shapes, including shapes with rectangular holes, under different loads. Hadjesfandiari and Dargush [9] investigated solution for two and three dimensional isotropic materials based on and couple stress theory and established a

_____
[*]Corresponding author.
E-mail address: sneh.mathematics@gmail.com (S.Yadav).

unique solution for displacement, rotation, and couple stresses. In addition to this, Hadjesfandiari and Dargush [10] analyzed different continuum mechanics theories such as couple stress theory, micro polar and strain-gradient theories. Taliercio and Veber [11] studied the effect of micro polar theory in orthotropic material with central axis of symmetry. They discussed three different cases for hollow cylinder under different conditions i.e. firstly, they analyzed hollow circular cylinder subjected to internal and external pressure with unlimited length. Secondly, they studied finite length hollow circular cylinder under the restriction of relative rotation of the base about its axis and finally, they analyzed twist in circular cylinder with axisymmetric configuration. They observed that results obtained for micro polar cylinder subjected to radial pressure are not significantly different from classical orthotropic cylinder. However, in case of twist the significant difference between classical and micro polar solutions has been observed. Further, Taliercio [12] presented analysis of twist in hollow solid cylinder made of linearly isotropic micro polar materials. Sharma et al. [13] studied torsion of a functionally graded thick-walled circular cylinder under internal and external pressure subjected to thermal loading using Seth transition theory.

In this paper, we have extended the work of Taliercio and Veber [14] for cylinder made up of orthotropic micro polar material and finite difference numerical algorithm has been used for analyzing shear stresses and couple stresses. A parametric study has been carried out to show the influence of different parameters i.e. characteristics length and material constants with a fixed orientation in hollow circular cylinders. Results have been discussed numerically with the help of graphs.

2   MATHEMATICAL FORMULATION

Consider a thick-walled hollow circular cylinder made up of orthotropic micro polar material whose internal and external radii are *a* and *b* respectively as shown in Fig. 1. A cylindrical coordinate system r, θ and z has been used where *z* lies in the longitudinal direction while *r* and θ lies in transverse direction of the cylinder.
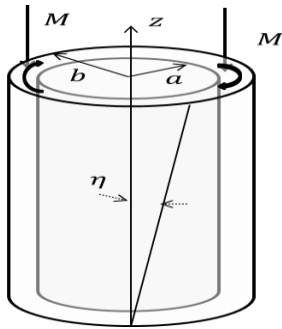

Fig.1
Hollow circular cylinder subjected to torsion.

The body forces and body moments are neglected, while the mechanical properties are assumed to be same throughout the cylinder. One end of the cylinder is assumed to be fixed at $z = 0$ while the other end of the cylinder i.e. $z = L$ (length of hollow cylinder) is rotating about *z*-axis with the fixed angle of twist η as shown in Fig. 1. In 3-dimensional continuum mechanics, six degree of freedom is required for each material point, three due to displacements and three due to rotations. Therefore, the component of macro displacement u and micro-rotation φ in curvilinear cylindrical coordinate (r, θ, z) for the second axially-symmetric problem depends on the space variables *r* and *z*, expressed as [15, 16]

$$u_r = 0, u_\theta = \eta r z, u_z = 0, \varphi_r = \eta \phi(r), \varphi_\theta = 0, \varphi_z = \eta z, \tag{1}$$

where u_r, u_θ, u_z are radial, circumferential and axial components of displacement respectively, while $\varphi_r, \varphi_\theta, \varphi_z$ are radial, circumferential and axial components of micro-rotation and $\phi(r)$ is an unknown function to be determined.

2.1 Basic equations

We have used deformation and constitutive equations given by Eringen [3, 17] on micro polar theory of elasticity. In the cylindrical coordinate system, the compatibility equations (micropolar strains and micro polar curvature in micro materials) are expressed as [11]

$$e_{ij} = u_{j,i} - e_{ijk}\varphi_k, \ \chi_{ij} = \varphi_{j,i} \ (i,j = 1,2,3),$$
(2)

where e_{ij}, χ_{ij}, u_j, φ_j are micro polar strains, micro-curvatures, displacements and micro-rotations respectively. In cylindrical coordinate system, these equations are explicitly expressed as:

$$e_{rr} = \frac{\partial u_r}{\partial r}, \ e_{\theta\theta} = \frac{1}{r}\left(\frac{\partial u_\theta}{\partial \theta} + u_r\right), \ e_{zz} = \frac{\partial u_z}{\partial z}, \ e_{r\theta} = \frac{\partial u_\theta}{\partial r} - \varphi_z,$$

$$e_{\theta r} = \frac{1}{r}\left(\frac{\partial u_r}{\partial \theta} - u_\theta\right) + \varphi_z, \ e_{\theta z} = \frac{1}{r}\frac{\partial u_z}{\partial \theta} - \varphi_r, \ e_{z\theta} = \frac{\partial u_\theta}{\partial z} + \varphi_r,$$

$$e_{zr} = \frac{\partial u_r}{\partial z} - \varphi_\theta, \ e_{rz} = \frac{\partial u_z}{\partial r} - \varphi_\theta, \ \chi_{rr} = \frac{\partial \varphi_r}{\partial r}, \ \chi_{\theta\theta} = \frac{1}{r}\left(\frac{\partial u_\theta}{\partial \theta} + \varphi_r\right),$$
(3)

$$\chi_{zz} = \frac{\partial \varphi_z}{\partial z}, \ \chi_{r\theta} = \frac{\partial \varphi_\theta}{\partial r}, \ \chi_{\theta r} = \frac{1}{r}\left(\frac{\partial \varphi_r}{\partial \theta} - \varphi_\theta\right), \ \chi_{\theta z} = \frac{1}{r}\frac{\partial \varphi_z}{\partial \theta},$$

$$\chi_{z\theta} = \frac{\partial \varphi_\theta}{\partial z}, \ \chi_{zr} = \frac{\partial \varphi_r}{\partial z}, \ \chi_{rz} = \frac{\partial \varphi_z}{\partial r}.$$

In this paper, we have considered second planar axially-symmetric problem therefore, Eq. (3) using Eq. (1) reduced to the form

$$e_{rr} = e_{\theta\theta} = e_{zz} = e_{r\theta} = e_{\theta r} = e_{zr} = e_{rz} = 0, \ e_{\theta z} = -\eta\phi(r), \ e_{z\theta} = \eta\{r + \phi(r)\},$$

$$\chi_{rr} = \eta\phi(r), \ \chi_{\theta\theta} = \eta\frac{\phi(r)}{r}, \ \chi_{zz} = \eta, \ \chi_{r\theta} = \chi_{\theta r} = \chi_{\theta z} = \chi_{z\theta} = \chi_{zr} = \chi_{rz} = 0.$$
(4)

The general constitutive equations in terms of stress, strain, couple stress tensors and micro curvatures are expressed as:

$$T_{ij} = A_{ijhk}e_{hk}, \ M_{ij} = B_{ijhk}\chi_{hk} \ (i,j,h,k = 1,2,3)$$
(5)

where A_{ijhk} and B_{ijhk} are fourth order elasticity tensors.

Due to two fold symmetry of orthotropic micro polar materials, we get the following relationship in material constants i.e. $A_{21} = A_{12}$, $A_{31} = A_{13}$, $A_{32} = A_{23}$, $A_{54} = A_{45}$, $A_{76} = A_{67}$, $A_{98} = A_{89}$.

Therefore, the stress-strain equations for orthotropic materials are written as:

$$T_{rr} = A_{11}e_{rr} + A_{12}e_{\theta\theta} + A_{13}e_{zz}, \ T_{\theta\theta} = A_{12}e_{rr} + A_{22}e_{\theta\theta} + A_{23}e_{zz},$$

$$T_{zz} = A_{13}e_{rr} + A_{23}e_{\theta\theta} + A_{33}e_{zz}, \ T_{r\theta} = A_{44}e_{r\theta} + A_{45}e_{\theta r},$$
(6)

$$T_{\theta r} = A_{45}e_{r\theta} + A_{55}e_{\theta r}, \ T_{\theta z} = A_{66}e_{\theta z} + A_{67}e_{z\theta},$$

$$T_{z\theta} = A_{67}e_{\theta z} + A_{77}e_{z\theta}, \ T_{zr} = A_{88}e_{zr} + A_{89}e_{rz}, \ T_{rz} = A_{89}e_{zr} + A_{99}e_{rz}.$$

Due to symmetry of micro polar materials, we get $B_{21} = B_{12}, B_{31} = B_{13}, B_{32} = B_{23}, B_{54} = B_{45}, B_{76} = B_{67}, B_{98} = B_{89}$.

Therefore, the constitutive equations for couple stresses and micro curvatures are expressed as:

$$M_{rr} = B_{11}\chi_{rr} + B_{12}\chi_{\theta\theta} + B_{13}\chi_{zz}, \ M_{\theta\theta} = B_{12}\chi_{rr} + B_{22}\chi_{\theta\theta} + B_{23}\chi_{zz},$$
$$M_{zz} = B_{13}\chi_{rr} + B_{23}\chi_{\theta\theta} + B_{33}\chi_{zz}, \ M_{r\theta} = B_{44}\chi_{r\theta} + B_{45}\chi_{\theta r},$$
$$M_{\theta r} = B_{45}\chi_{r\theta} + B_{55}\chi_{\theta r}, \ M_{\theta z} = B_{66}\chi_{\theta z} + B_{67}\chi_{z\theta},$$
$$M_{z\theta} = B_{67}\chi_{\theta z} + B_{77}\chi_{z\theta}, M_{zr} = B_{88}\chi_{zr} + B_{89}\chi_{rz}, \ M_{rz} = B_{89}\chi_{zr} + B_{99}\chi_{rz}, \tag{7}$$

where A_{ij} and B_{ij} $(i,j = 1,2,3,...,9)$ are known as orthotropic micro polar material constants. Using Eqs. (4), (6) and (7) can be written as:

$$T_{\theta z} = -A_{66}\eta\phi(r) + A_{67}\eta[r + \phi(r)], \ T_{z\theta} = -A_{67}\eta\phi(r) + A_{77}\eta[r + \phi(r)],$$
$$M_{rr} = B_{11}\eta\phi'(r) + B_{12}\eta\frac{\phi(r)}{r} + B_{13}\eta, \ M_{\theta\theta} = B_{21}\eta\phi'(r) + B_{22}\eta\frac{\phi(r)}{r} + B_{23}\eta,$$
$$M_{zz} = B_{31}\eta\phi'(r) + B_{32}\eta\frac{\phi(r)}{r} + B_{33}\eta, \tag{8}$$
$$T_{rr} = T_{\theta\theta} = T_{zz} = T_{r\theta} = T_{\theta r} = T_{zr} = T_{rz} = M_{r\theta} = M_{\theta r} = M_{\theta z} = M_{z\theta} = M_{zr} = M_{rz} = 0.$$

In the absence of body force and moment force, the equilibrium equations are expressed as:

$$T_{ij,i} = 0, \ M_{ij,i} + e_{jhk}T_{hk} = 0, \quad (i,j = 1,2,3), \tag{9}$$

where T_{ij}, M_{ij} are stresses, couple stresses and e_{jhk} is called permutation tensor. In curvilinear cylindrical system, equilibrium equations in the absence of body force and body moment are written as [11]

$$\frac{\partial T_{rr}}{\partial r} + \frac{1}{r}\frac{\partial T_{\theta r}}{\partial \theta} + \frac{\partial T_{zr}}{\partial z} + \frac{T_{rr} - T_{\theta\theta}}{r} = 0, \ \frac{\partial T_{r\theta}}{\partial r} + \frac{1}{r}\frac{\partial T_{\theta\theta}}{\partial \theta} + \frac{\partial T_{z\theta}}{\partial z} + \frac{T_{\theta r} + T_{r\theta}}{r} = 0,$$
$$\frac{\partial T_{rz}}{\partial r} + \frac{1}{r}\frac{\partial T_{\theta z}}{\partial \theta} + \frac{\partial T_{zz}}{\partial z} + \frac{T_{rz}}{r} = 0, \ \frac{\partial M_{rr}}{\partial r} + \frac{1}{r}\frac{\partial M_{\theta r}}{\partial \theta} + \frac{\partial M_{zr}}{\partial z} + \frac{M_{rr} - M_{\theta\theta}}{r} + T_{\theta z} - T_{z\theta} = 0,$$
$$\frac{\partial M_{r\theta}}{\partial r} + \frac{1}{r}\frac{\partial M_{\theta\theta}}{\partial \theta} + \frac{\partial M_{z\theta}}{\partial z} + \frac{M_{\theta r} + M_{r\theta}}{r} + T_{zr} - T_{rz} = 0, \tag{10}$$
$$\frac{\partial M_{rz}}{\partial r} + \frac{1}{r}\frac{\partial M_{\theta z}}{\partial \theta} + \frac{\partial M_{zz}}{\partial z} + \frac{M_{rz}}{r} + T_{r\theta} - T_{\theta r} = 0.$$

Using Eq. (8) in Eq. (10), we have

$$\frac{dM_{rr}}{dr} + \frac{M_{rr} - M_{\theta\theta}}{r} + T_{\theta z} - T_{z\theta} = 0. \tag{11}$$

Substituting Eq. (8) in Eq. (11), we will obtain a second order differential equation in terms of stress function $\phi(r)$ expressed as:

$$B_{11}r^2\phi''(r) + B_{11}r\phi'(r) + \left[-B_{22} + r^2(2A_{67} - A_{66} - A_{77})\right]\phi(r) = r(B_{23} - B_{13}) + r^3(A_{77} - A_{67}) \tag{12}$$

Since thick-walled circular cylinder considered is hollow therefore, the boundary conditions for Eq. (12) are defined as:

$$M_{rr} = 0 \text{ at } r = a \text{ and } M_{rr} = 0 \text{ at } r = b, \tag{13}$$

where M_{rr} is couple stress, a and b are internal and external radii of the circular hollow cylinder.

Boundary conditions in terms of stress function $\phi(r)$ can be written as:

$$B_{11}\eta\phi'(a) + B_{12}\eta\frac{\phi(a)}{a} + B_{13}\eta = 0, \quad B_{11}\eta\phi'(b) + B_{12}\eta\frac{\phi(b)}{b} + B_{13}\eta = 0 \tag{14}$$

To normalize the differential Eq. (11), the following components are defined in non-dimensional form as:

$$R = \frac{r}{b}, \; R_0 = \frac{a}{b}, \; \overline{A_{ij}} = \frac{A_{ij}}{A_{11}} \; (i,j = 6,7), \; \overline{B_{ij}} = \frac{B_{ij}}{l_i^2 A_{77}} \; (i,j = 1,2), \; \overline{\lambda_i} = \frac{l_i}{b}, \; \psi = \frac{\phi}{b}, \; \sigma_{z\theta} = \frac{T_{z\theta}}{A_{77}R\eta},$$

$$\sigma_{\theta z} = \frac{T_{\theta z}}{A_{77}R\eta}, \; m_{rr} = \frac{M_{rr}}{A_{77}R^2\eta}, \; m_{\theta\theta} = \frac{M_{\theta\theta}}{A_{77}R^2\eta}, \; m_{zz} = \frac{M_{zz}}{A_{77}R^2\eta},$$

where r is radius of the cylinder, A_{77} is shear modulus and l_i is the internal length of micro orthotropic material. Boundary value problem defined in Eqs. (12) and (14) in non-dimensional form can be written as:

$$\overline{B_{11}}R^2\psi''(r) + \overline{B_{11}}R\psi'(r) + \left[-\overline{B_{22}} + \left(\frac{R}{\overline{\lambda_i}}\right)^2 \left(2\overline{A_{67}} - \overline{A_{66}} - \overline{A_{77}}\right) \right]\psi(r) = R\left(\overline{B_{23}} - \overline{B_{13}}\right) + R^3\left(\overline{A_{77}} - \overline{A_{67}}\right) \tag{15}$$

and

$$\overline{B_{11}}\psi'(R_0) + B_{12}\frac{\psi(R_0)}{R_0} + \overline{B_{13}} = 0, \; \overline{B_{11}}\psi'(1) + \overline{B_{12}}\psi(b) + \overline{B_{13}} = 0. \tag{16}$$

The torsion in the cylinder is given by

$$T_{or} = \int_A \eta\left(rT_{z\theta} + M_{zz}\right)dA \tag{17}$$

The boundary value problem given by Eqs. (15) and (16) has been solved with the finite difference algorithm. After computing function ψ, we determined shear stresses and couple stresses using Eq. (8).

3 RESULTS AND NUMERICAL DISCUSSION

To illustrate the influence of material parameters and internal length on twisted hollow circular cylinder, Figs. 2(a)-(b) have been drawn between stress function and radii ratio.

Fig. 2(a) shows the effect of internal length ratio $\overline{\lambda_i}$ on the stress function for fixed value of orthotropic material constants. It is noticed that stress function is linear throughout the radii with different slopes and changes in value of stresses is noticeable when values of internal length ratio switches from $\overline{\lambda_i} = 0.1$ to $\overline{\lambda_i} = 1$.

Fig. 2(b) shows the effect of material constants $\overline{A_{66}} = 0.2, 0.5, 0.7, 1$. It has been observed that stress function is very close to zero at the internal radii and approximately linear for $\overline{A_{66}} = 1$. With the decrease in value of $\overline{A_{66}}$, stress function moves away from zero at internal radii and behavior of stress function is linear throughout the radii. To observe the effect of orthotropic material constants with different material internal lengths on shear stresses, curves have been drawn between radii ratio and shear stresses.
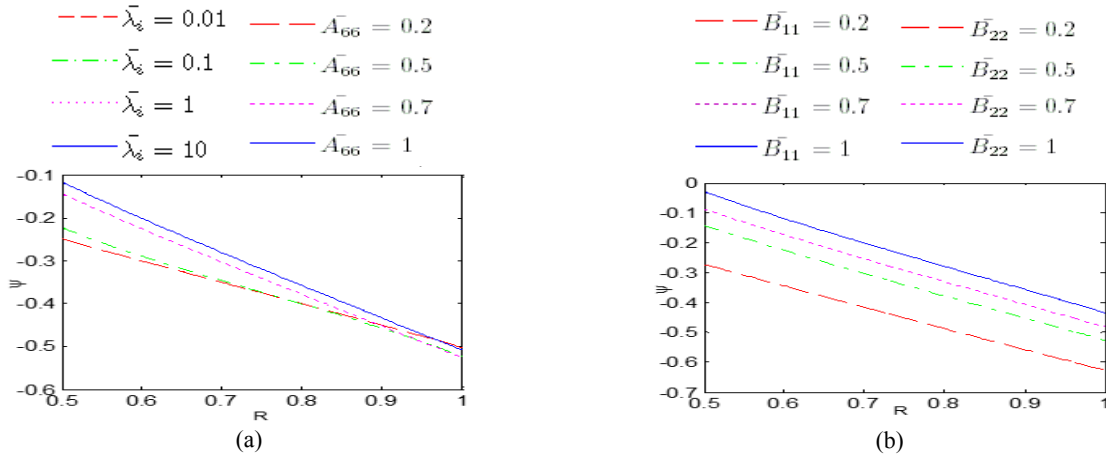
Fig.2
Stress function: (a) influence of internal length $\overline{\lambda}_i = 0.01, 0.1, 1, 10$ (b) influence of material constant $\overline{A}_{66} = 0.2, 0.5, 0.7, 1$.

Figs. 3(a)–(c) have been drawn between radii ratio and shear stresses $(\sigma_{z\theta})$ to shows the influence of materials constant $\overline{A}_{66} = 0.2, 0.5, 0.7, 1$ on shear stresses with fixed internal length $\overline{\lambda}_i = 1, 0.1, 0.01$. Fig. 3(a) shows the effect of material constant $\overline{A}_{66} = 0.2, 0.5, 0.7, 1$ with $\overline{\lambda}_i = 1$ on shear stresses. It is noticed that shear stresses are maximum for $\overline{A}_{66} = 1$ and minimum for $\overline{A}_{66} = 0.2$. Also, these stress decreases with the decrease in internal length as can be seen in Fig. 3(b). With the change in internal length from $\overline{\lambda}_i = 0.1$ to $\overline{\lambda}_i = 0.01$, it is noticed from Fig. 3(c) that the effect of material constant is negligible.

To show the effect of material constant $\overline{B}_{11}$ and $\overline{B}_{22}$ on shear stresses respectively, the larger value of $\overline{\lambda}_i$ is considered as can be seen from Figs. 3(d)-3(e). From Fig. 3(d), it has been observed that shear stresses are nonlinear. These stresses are maximum at internal surface for $\overline{B}_{11} = 0.2$ and at external surface for other values of $\overline{B}_{11}$. It has been observed from Fig. 3(e) that shear stresses are linear in nature and are maximum at external surface for all values of $\overline{B}_{22}$ except for $\overline{B}_{22} = 0.2$ for which these shear stresses are minimum. Fig. 3(f) shows the influence of different internal lengths with fixed material constants. With the decrease in internal length, shear stresses decreases.
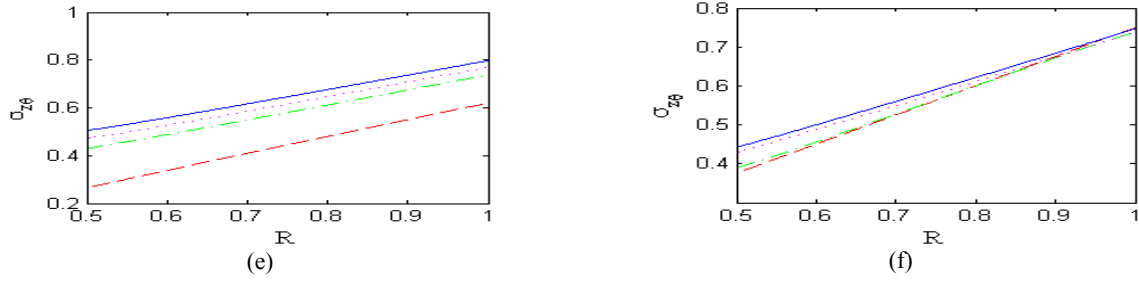
(e)   (f)
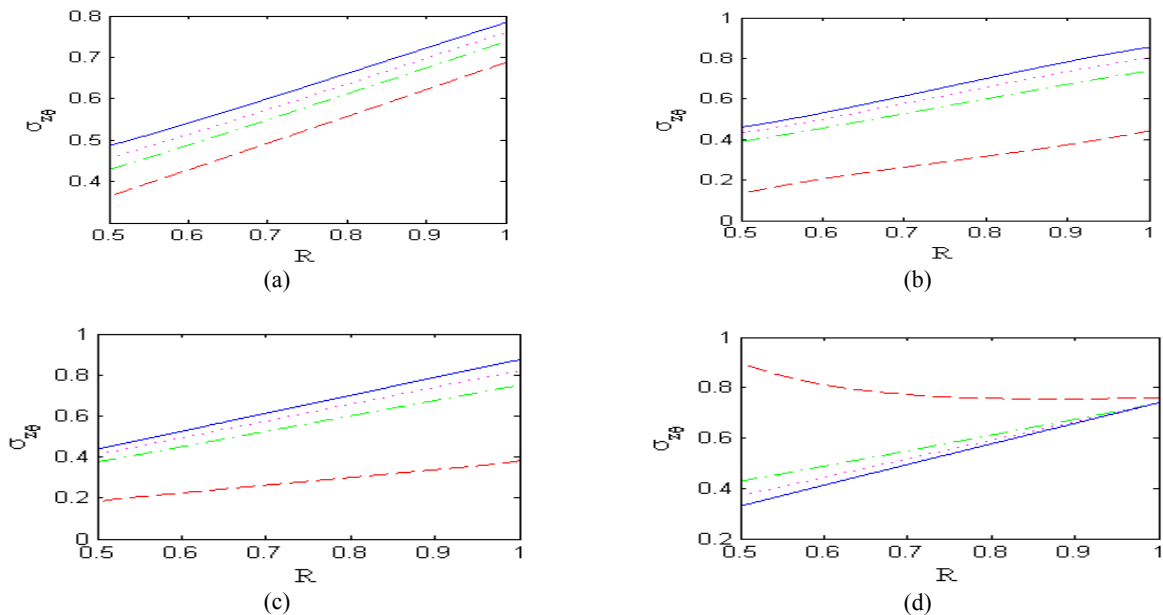
Fig.3

Shear stress $\sigma_{z\theta}$: (a) influence of $\overline{A_{66}}$ with internal length $\overline{\lambda_i}=1$ (b) influence of $\overline{A_{66}}$ with internal length $\overline{\lambda_i}=0.1$ (c) influence of $\overline{A_{66}}$ with internal length $\overline{\lambda_i}=0.01$ (d) influence of $\overline{B_{11}}$ with internal length $\overline{\lambda_i}=1$ (e) influence of $\overline{B_{22}}$ with internal length $\overline{\lambda_i}=1$ (f) influence of internal length $\overline{\lambda_i}$ with $\overline{A_{66}}=0.5$.

As material is micro polar, so $\sigma_{z\theta}$ is not symmetric to $\sigma_{\theta z}$ therefore, Figs. 4(a)-(d) have been drawn between $\sigma_{\theta z}$ and radii ratio to observe the effect of internal length and orthotropic micro polar material constants on shears stresses.

Figs. 4(a)-(c) shows the sensitivity of material constant $\overline{A_{66}}$ with different values of material internal lengths $\overline{\lambda_i}=1, 0.1, 0.01$ on shear stresses. From Fig. 4(a), it is observed that shear stresses are maximum at external surface for $\overline{A_{66}}=1$. It has also been observed that with the decrease in internal length from $\overline{\lambda_i}=0.1$ to $\overline{\lambda_i}=0.01$, there is very small effect of material constant $\overline{A_{66}}$ on shear stresses as can be seen from Figs. 4(b) and 4(c). From Fig. 4(d), it has been noticed that shear stress $\sigma_{\theta z}$ are maximum at external surface and theses shear stresses $\sigma_{\theta z}$ are high as compared to shear stresses $\sigma_{z\theta}$. Also, it is noticed that shear stress $\sigma_{z\theta}$ is maximum for $\overline{A_{66}}=1$ while shear stress $\sigma_{\theta z}$ is maximum for $\overline{A_{66}}=0.2$.
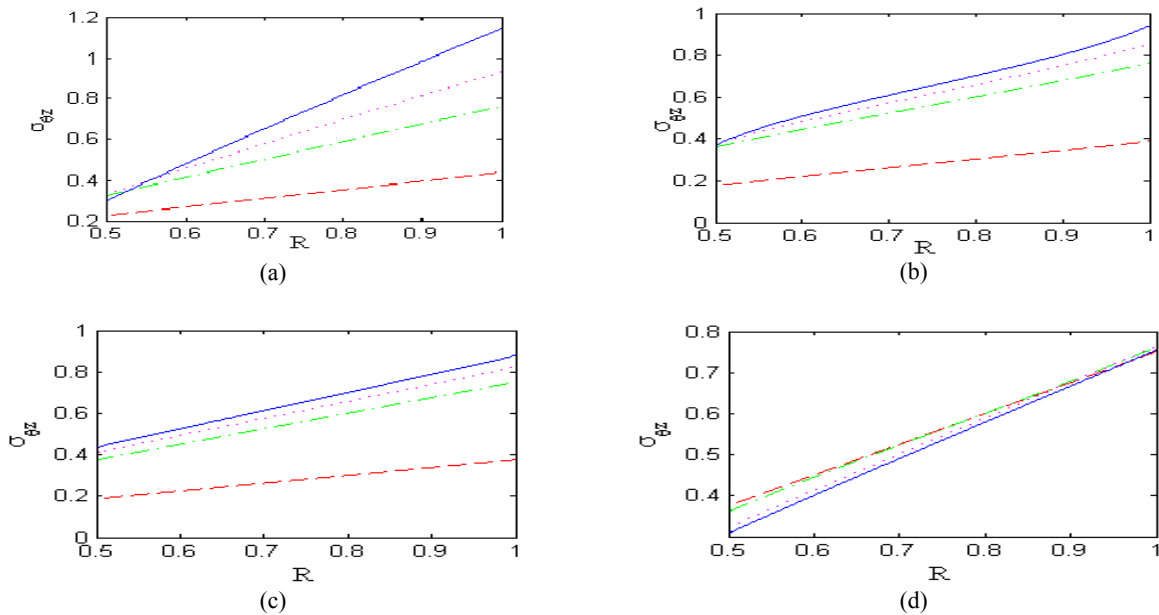

(a)   (b)

(c)   (d)

Fig.4

Shear stress $\sigma_{\theta z}$: (a) influence of $\overline{A_{66}}$ with internal length $\overline{\lambda_i}=1$ (b) influence of $\overline{A_{66}}$ with internal length $\overline{\lambda_i}=0.1$ (c) influence of $\overline{A_{66}}$ with internal length, $\overline{\lambda_i}=0.01$ (d) influence of internal length $\overline{\lambda_i}$ with $\overline{A_{66}}=0.5$.

Radial couple stresses have been drawn in Figs. 5(a)–(e) to show the influence of material constant $\overline{A}_{66}$ with $\overline{\lambda}_i = 1, 0.1, 0.01$ on couple stresses. It is observed from Fig. 5(a) and 5(b) that couple stress increases with the change in internal length from $\overline{\lambda}_i = 1$ to $\overline{\lambda}_i = 0.1$. Also, it is noticed that the behavior of radial couple stresses at $\overline{A}_{66} = 0.5, 0.7, 1$ is opposite to $\overline{A}_{66} = 0.2$. It has been observed from Fig. 5(c) that radial couple stresses are constant for small internal length $\overline{\lambda}_i = 0.01$ except near the boundary of the cylinder. From Fig. 5(d), it is found that radial couple stresses are compressive for $\overline{B}_{11} = 1$. From Fig. 5(e), it is observed that for $\overline{B}_{22}$ radial couple stresses are tensile and increases with the increase in the value of $\overline{B}_{22}$. Radial couple stress is maximum for higher value of internal length as can be noticed from Fig. 5(f). Also, it has been noticed that effect of smallest internal length on radial couple stresses is negligible.
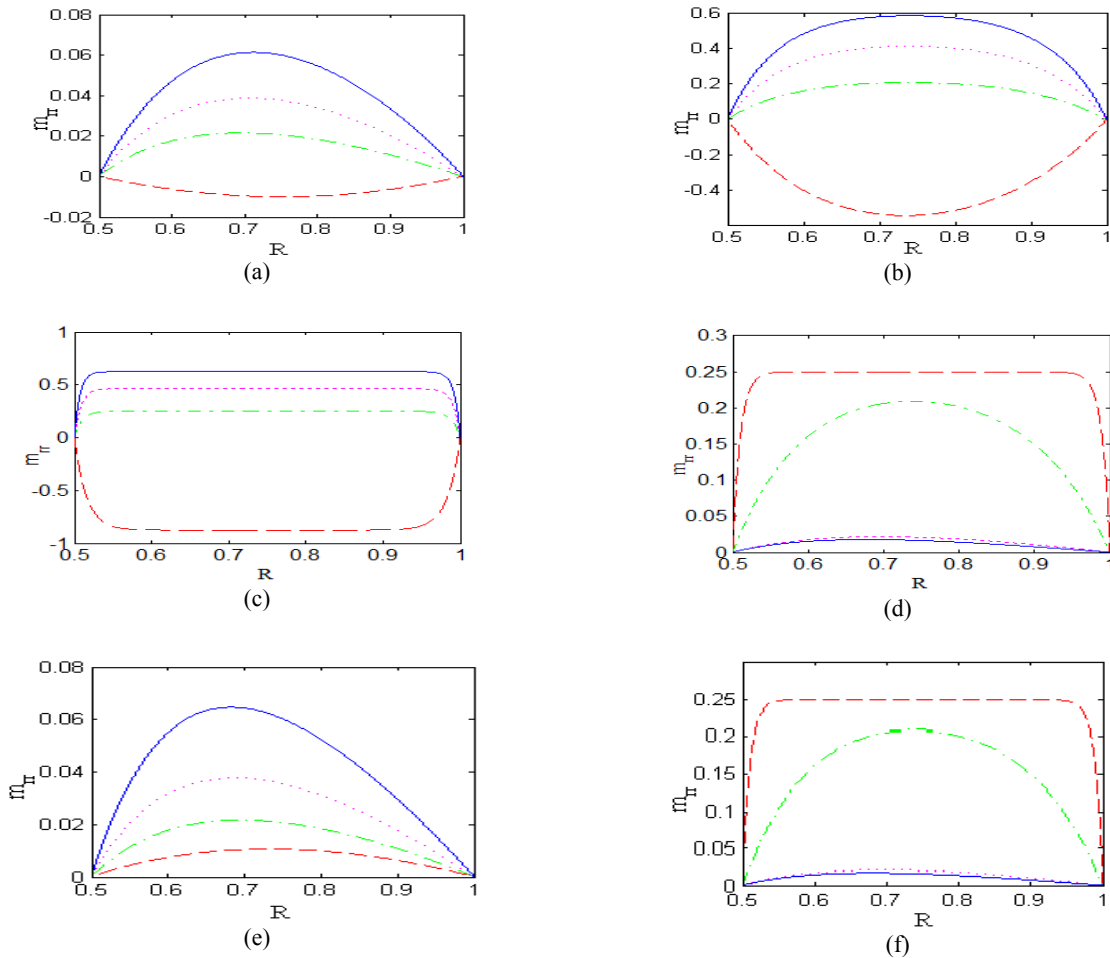

Fig.5
Couple stress m_{rr} : (a) influence of $\overline{A}_{66}$ with internal length, $\overline{\lambda}_i = 1$ (b) influence of $\overline{A}_{66}$ with internal length $\overline{\lambda}_i = 0.1$ (c) influence of $\overline{A}_{66}$ with internal length $\overline{\lambda}_i = 0.01$ (d) influence of internal length $\overline{\lambda}_i$ with $\overline{A}_{66} = 0.5$ (e) influence of $\overline{B}_{11}$ with internal length $\overline{\lambda}_i = 1$ (f) influence of $\overline{B}_{22}$ with internal length $\overline{\lambda}_i = 1$.

Circumferential couple stresses have been drawn in Figs. 6(a)-(d) to show the effect of material parameters $\overline{A}_{66}$ with different values of internal length $\overline{\lambda}_i = 1, 0.1, 0.01$ on circumferential couple stresses. Fig. 6(a) and 6(b) shows that the circumferential couple stresses are maximum for $\overline{A}_{66} = 1$. Also, these circumferential couple stresses are constant except near the boundary of the cylinder for $\overline{\lambda}_i = 0.01$ as can be seen from Fig. 6(c). Fig. 6(d) shows

the influence of internal length with fixed material constants on circumferential couple stresses. Also, it is noticed that for smallest value of internal length, these couple stresses are constant throughout the radii ratio except at free boundaries. Also, behavior of circumferential couple stresses for largest internal length, i.e. $\overline{\lambda_i} = 10, 1$ varies differently as compared to smallest internal length i.e. $\overline{\lambda_i} = 0.1, 0.01$.
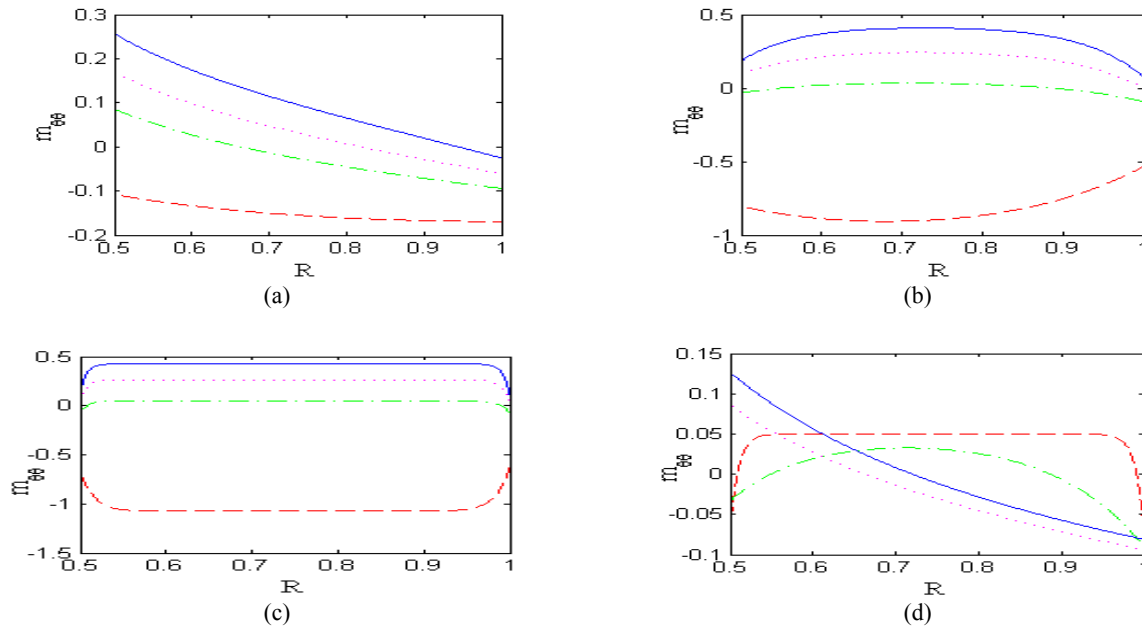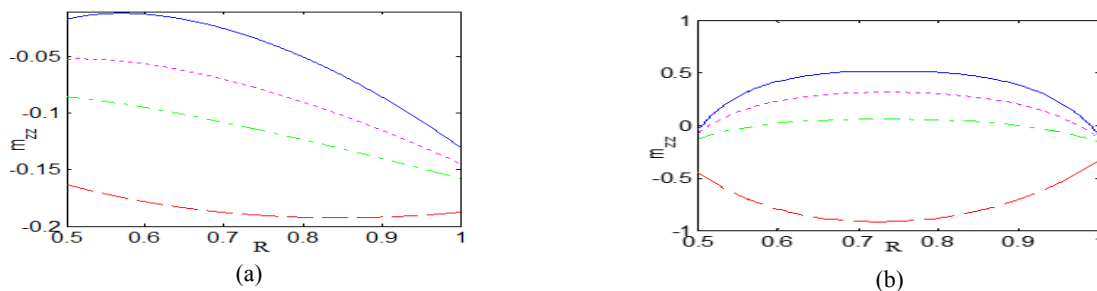

Fig.6

Couple stress $m_{\theta\theta}$: (a) influence of $\overline{A_{66}}$ with internal length $\overline{\lambda_i} = 1$ (b) influence of $\overline{A_{66}}$ with internal length $\overline{\lambda_i} = 0.1$ (c) influence of $\overline{A_{66}}$ with internal length $\overline{\lambda_i} = 0.01$ (d) influence of internal length, $\overline{\lambda_i}$ with $\overline{A_{66}} = 0.5$.

Figs. 7(a)–(d) have been drawn for axial couple stress with radii ratio with different values of $\overline{A_{66}}$ and internal length $\overline{\lambda_i} = 1, 0.1, 0.01$. It is observed from Fig. 7(a) and Fig. 7(b) that these axial couple stresses are maximum at internal surface for $\overline{A_{66}} = 1$ at $\overline{\lambda_i} = 1$ and $\overline{\lambda_i} = 0.1$. However, it is found from Fig. 7(c) that these couple stresses are constant throughout the radii except free boundaries for small internal length $\overline{\lambda_i} = 0.01$. Fig. 7(d) shows the influence of various internal lengths $\overline{\lambda_i} = 10, 1, 0.1, 0.01$ on axial couple stresses with fixed angle of twist and material constants. It has been noticed that effect of larger value of internal length i.e. $\overline{\lambda_i} = 10$ on axial couple stress is negligible. The code of the algorithm has been compiled and executed in MATLAB running on a PC.
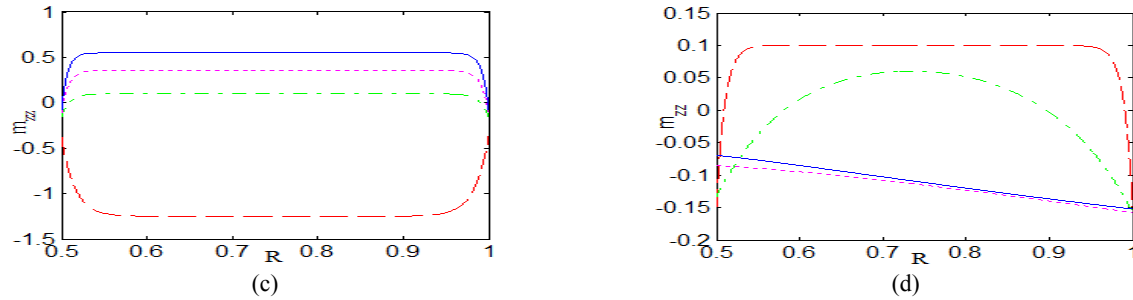
Fig.7

Couple stress m_{zz} : (a) influence of $\overline{A_{66}}$ with internal length $\overline{\lambda_i} = 1$ (b) influence of $\overline{A_{66}}$ with internal length $\overline{\lambda_i} = 0.1$ (c) influence of $\overline{A_{66}}$ with internal length $\overline{\lambda_i} = 0.01$ (d) influence of internal length $\overline{\lambda_i}$ with $\overline{A_{66}} = 0.5$.

4   CONCLUSIONS

Using finite difference method, numerical solution in terms of stresses, couple stresses and micro-rotations have been obtained. Our results are good in agreement with Taliercio and Veber [14], for hollow circular cylinder made up of isotropic material. It has been concluded that the effect of smallest internal length on both kind of shear stresses $\sigma_{z\theta}$ and $\sigma_{\theta z}$ is negligible. Moreover, the couple stresses are constant throughout the radii for hollow circular cylinder except at free boundaries and in small neighborhood of these boundaries when internal length is small. Couple stresses showing its significance for materials whose internal length is large.

REFERENCES

[1]   Pagano N.J., Sih G.C., 1968, Stress singularities around a crack in a cosserat plate, *International Journal of Solids and Structures* **4**(5): 531-553.
[2]   Fatemi J., Onck P.R., Poort G., van Keulen F., 2003, Cosserat moduli of anisotropic cancellous bone: A micromechanical analysis, *Journal de Physique IV* **105**: 273-280.
[3]   Eringen A.C., 1966, Linear theory of micropolar elasticity, *Journal of Mathematics and Mechanics* **15**: 909-923.
[4]   Eringen A.C., 1999, *Microcontinuum Field Theories*, Springer, Berlin edition.
[5]   Altenbach H., Eremeyev V.A., 2010, Thin-walled structures made of foams, *Cellular and Porous Materials in Structures and Processes* **2010**: 167-242.
[6]   Gauthier R.D., Jahsman W.E., 1975, A quest for micropolar elastic constants, *Journal of Applied Mechanics* **42**(2): 369-374.
[7]   Merkel A., Tournat V., Gusev V., 2011, Experimental evidence of rotational elastic waves in granular phononic crystals, *Physical Review Letters* **107**(22): 225502.
[8]   Kvasov R., Steinberg L., 2013, Numerical modeling of bending of micropolar plates, *Thin-Walled Structures* **69**: 67-78.
[9]   Hadjesfandiari A.R., Dargush G.F., 2014, Evolution of generalized couple-stress continuum theories: A critical analysis, *Physics* **2014**:1501.03112.
[10]   Hadjesfandiari A.R., Dargush G.F., 2013, Fundamental solutions for isotropic size-dependent couple stress elasticity, *International Journal of Solids and Structures* **50**(9): 1253-1265.
[11]   Taliercio A., Veber D., 2009, Some problems of linear elasticity for cylinders in micropolar orthotropic material, *International Journal of Solids and Structures* **46**(22): 3948-3963.
[12]   Taliercio A., 2010, Torsion of micropolar hollow circular cylinders, *Mechanics Research Communications* **37**(4): 406-411.
[13]   Sharma S., Yadav S., Sharma R., 2015, Thermal creep analysis of functionally graded thick-walled cylinder subjected to torsion and internal and external pressure, *Journal of Solid Mechanics* **9**(2): 302-318.
[14]   Taliercio A., Veber D., 2016, Torsion of elastic anisotropic micropolar cylindrical bars, *European Journal of Mechanics-A/Solids* **55**: 45-56.
[15]   Smith A., 1970, Torsion and vibrations of cylinders of a micropolar elastic solid, *Recent Advances in Engineering Science* **5**:129-137.
[16]   Reddy G.V.K., Venkatasubramanian N.K., 1976, Saint-venant's problem for a micropolar elastic circular cylinder, *International Journal of Engineering Science* **14**(11): 1047-1057.
[17]   Eringen A.C., 1968,*Theory of Micropolar Elasticity*, New York, Academic Press.